



**HAL**  
open science

## Observation of plastic deformation wave in a tensile-loaded aluminum-alloy

S Yoshida, B Siahaan, H. Pardede, N. Sijabat, H. Simangunsong, T. Simbolon, A. Kusnowo

► **To cite this version:**

S Yoshida, B Siahaan, H. Pardede, N. Sijabat, H. Simangunsong, et al.. Observation of plastic deformation wave in a tensile-loaded aluminum-alloy. *Physics Letters A*, 1999, 251 (1), pp.54 - 60. hal-01092645

**HAL Id: hal-01092645**

**<https://hal.science/hal-01092645>**

Submitted on 9 Dec 2014

**HAL** is a multi-disciplinary open access archive for the deposit and dissemination of scientific research documents, whether they are published or not. The documents may come from teaching and research institutions in France or abroad, or from public or private research centers.

L'archive ouverte pluridisciplinaire **HAL**, est destinée au dépôt et à la diffusion de documents scientifiques de niveau recherche, publiés ou non, émanant des établissements d'enseignement et de recherche français ou étrangers, des laboratoires publics ou privés.

# Observation of plastic deformation wave in a tensile-loaded aluminum-alloy

S. Yoshida, B. Siahaan, M. H. Pardede, N. Sijabat, H. Simangunsong, T. Simbolon, A. Kusnowo

Research and Development Center for Applied Physics,

Indonesian Institute of Sciences

P3FT-LIPI, PUSPIPTEK, Serpong, Tangerang 15310, Indonesia

Phone:62-21-756-0570, Fax: 62-21-756-0554, E-mail: yoshida@phys.ufl.edu

Present address: University of Florida, Department of Physics,

POB 118440, Gainesville, Fl 32611

A displacement wave has been observed in a plastically deforming aluminum-alloy sample under a tensile load. The observed wave indicates a recently proposed mechanism concerning how deformation evolves to fracture. The estimated phase velocity of 110 mm/min is three orders of magnitude higher than the tensile speed.

To understand the plastic deformation (PD) properly is important not only for scientific interest but also for various applications such as strength assessment of solid-state structures and development of new materials. Recently Panin et al. [1] have developed a theory of plastic deformation called mesomechanics. Using a transformation of  $GL(3, R)$  group to describe deformation of a local-bench-mark (LBM) set up in a deformation structure element (DSE), and requesting the local symmetry to make the Lagrangian invariant, mesomechanics has introduced a gauge field and derived a field equation [2]. This leads to a set of equations analogous to the Maxwell equation of electromagnetism [1,7], which describes the synergetic interaction between the translational and rotational modes of displacement (translational-rotational interaction, TRI). Physically, this dynamics represents the process of stress relaxation in a dissipative medium. Thus, according to mesomechanics, the PD is a self-organized wave phenomenon, and the associated waves are inclusively called the plastic deformation wave (PDW). After summation over the group indices, the following wave equation governing the translational component of the displacement field can be obtained.

$$\nabla^2 V - \frac{1}{c_t^2} \frac{\partial^2 V}{\partial t^2} = \frac{\partial}{\partial t} \left( g^{ij} \eta_i^\alpha \frac{D\eta_j^\alpha}{l^{2D_f}} \right) - \nabla \cdot (g^{ij} \eta_i^\alpha \dot{\eta}_j^\alpha). \quad (1)$$

where  $V(u, v)$  is the rate of displacement,  $c_t$  is the phase velocity,  $\omega$  is the angle of rotation,  $g^{ij}$  is the metric tensor,  $\eta_i$  is the LBM,  $l$  is the parameter representing the scale-level,  $D_f$  is the fractal dimension,  $i$  and  $j$  are the internal indices and  $\mu$  denotes the external indices. The first term in the right hand side represents the velocity of rotation of the DSE and the second term represents the source of the translational flow (such as a defect flow). Because of the spatial non-uniformity, the displacement field shows vortical characters called the translational-rotational vortex (TRV).

One of the strengths of mesomechanics is its capability of describing all the stages of PD including the fracture on the same theoretical basis. This feature enables one to predict a fracture in the PD stage. According to this theory [1,3], PD develops through a hierarchy of scale-levels (micro-, meso- and macro-level). When the scale-level is low, the stress

relaxes through the TRI. As the PD develops and its scale-level grows, the TRI mechanism becomes less effective causing the PDW to decay, and the strain tends to be localized (strain localization). The fracture is interpreted as the stage of PD when the TRI stops operating and the PD becomes characterized only by the rotational mode (fracture criterion). In this stage, the stress cannot be relaxed by the propagation of a PDW but by the generation and development of discontinuity (i.e., a crack). This situation is preceded by pre-fracture criteria observed in the PDW and TRV [4]: the wavelength of the PDW grows to be comparable to the sample size (wavelength criterion), the PDW stops traveling (standing wave criterion) and a band structure [8] appears at the boundary of a pair of developed TRVs (TRV criterion). Thus the temporal variation of the PDW provides essential information that indicates how the PD evolves to a fracture and in what stage of PD the material currently undergoes. The fracture criterion can be satisfied in any scale-level; if it is satisfied in a low level, the discontinuous situation is potentially recoverable [9] and the sample will not fail, but if it is satisfied in the macro-level it leads to a failure.

Previously, a number of experiments demonstrated various wave characteristics of PD. These include observations of grain rotations and TRV-like shapes of deformed grains [1,3], spatial and temporal wave characteristics in distortion (shear and normal strains  $\epsilon_{xy}$ ,  $\epsilon_{xx}$  and rotation  $\omega_z$ ) [1,3,6,7], vortices in displacement fields [1,3,5], and the wavelength and standing wave criteria observed in distortion-waves [1,4,10]. More recently, we have discovered that the above-mentioned band structure can be visualized as an optical interferometric band-pattern (called the white band, WB) [11]. We have found that the WB is dynamic on the sample surface until the degree of stress concentration reaches a certain level, and that depending on the stress condition, the WB can be classified into three types: move-and-stay (MS), stay-stationary (SS), and late-start (LS) types [12]. In any case, the sample always fails at the location where the WB becomes stationary, implying the standing wave criterion.

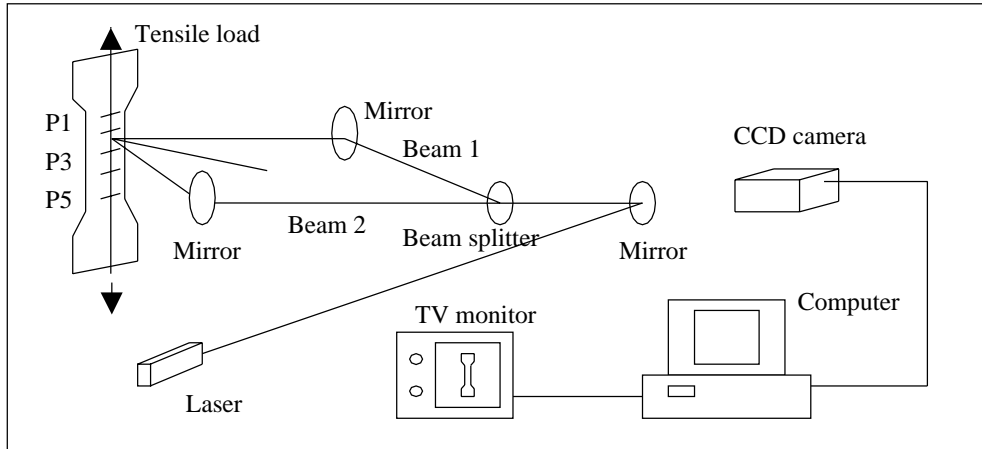
In this study, we investigate the wave characteristic of PD observed in a displacement field, rather than in the distortion. In our opinion, from the facts that the above-mentioned Maxwell-like equations are directly derived from the field equation and that these equations describe the relationship between the translational and rotational modes of displacement, the displacement is the primary quantity that represents the wave characteristics of PD. Therefore, it is important to observe a displacement-wave and analyze it for its spatial and temporal characteristics, as well as to observe a distortion-wave which represents the dynamics of stress concentration. Note that having different physical dimensions, the displacement and distortion potentially represent different aspects of the same PD as a self-organized wave.

Thus we gave a tensile load to aluminum-alloy samples at various loading speeds and monitored the displacement continuously until the sample failed. The results show clear wave characteristics of the displacement field. In some cases, to our surprise, the observed PDW shows rather simple decaying characteristics indicating the pre-fracture behavior described by mesomechanics. In this paper we report on these observations and discuss them based on mesomechanics. We also interpret the observations from the viewpoint of the fluctuation dissipation theorem. This helps us understand the mesomechanical description of PD and fracture more intuitively.

We measured displacement by electronic speckle-pattern interferometry [13]. We analyzed the horizontal component

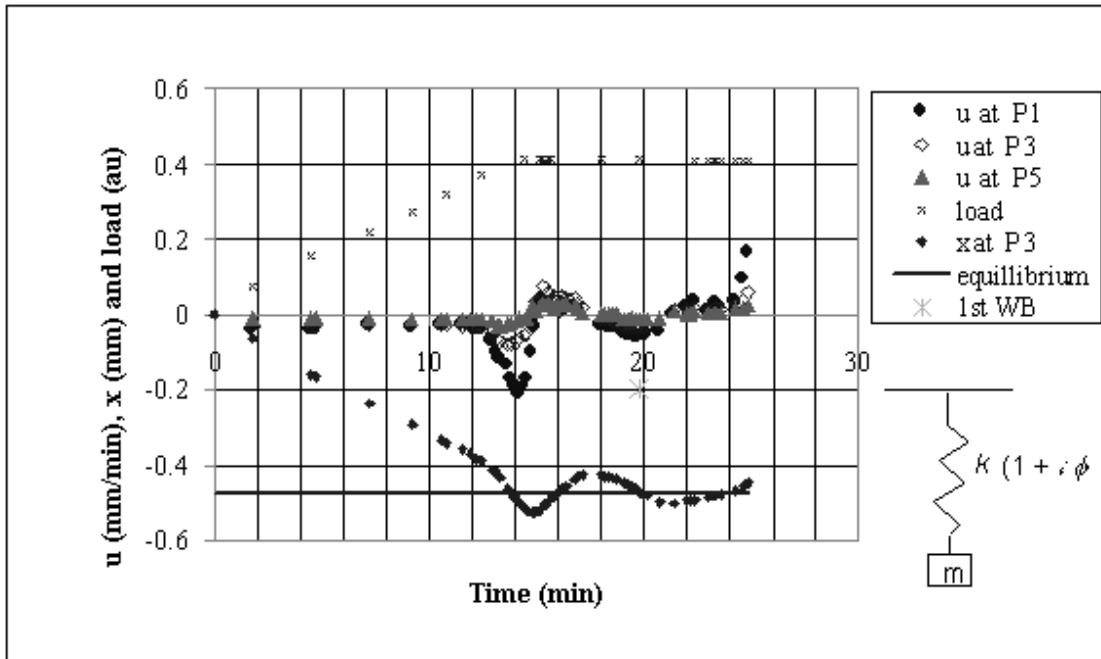
( $u$ ), since it does not contain the dc term associated with the motion of the tensile machine's head and therefore reveals the wave characteristics more clearly than the vertical component. Fig. 1 illustrates the experimental setup. The optical arrangement is a standard, in-plane sensitive configuration [14]. The sample is an aluminum-alloy (A6063) plate of 200 mm long (100 mm in effective length), 25 mm wide and 1 mm thick. The grain size of this material is estimated to be approximately  $150 \mu\text{m}$ . We gave a tensile load at a constant head speed ranging from 0.1 to 1 mm/min (hereafter referred to as the tensile speed). At each time step, we took a pair of specklegrams with a deformation interval appropriate for obtaining a reasonable number of interferometric fringes. We extracted  $u$  at five reference points along the central, vertical axis of the sample (Fig. 1).

FIG. 1. Experimental Setup.



The wave characteristics of  $u$  (called the  $u$ -wave) were most clearly observed in samples showing an LS type WB. Fig. 2 shows the  $u$ -wave extracted from one of these samples together with the loading characteristics. The tensile speed for this measurement was 0.1 mm/min. For clarity, only the  $u$ -waves extracted at the highest, middle and lowest reference points (P1, P3 and P5) are plotted. Also shown in Fig. 2 is the time historical trace of the middle point P3 ( $x$ -wave) evaluated by numerically integrating the  $u$ -wave with respect to time. The following features are observed: the  $u$ -wave starts rising when the stress reaches about 85% of the proof stress (stress at the yield point); the  $u$ -wave shows the maximum peak around the yield point; around this peak, a phase delay is observed among different reference points indicating that the  $u$ -wave travels upward; as the deformation progresses, the phase delay fades out and the  $u$ -wave comes to show only the temporal oscillation; the amplitude of this temporal oscillation decays monotonically until the sample fails, and its period tends to increase; and towards the failure, the temporal oscillation fades out completely. These features are commonly observed in all the samples that showed an LS type WB except that in one case the  $u$ -wave travels downward and in other cases a small peak appears prior to the maximum peak around the yield point. Below, noting these features, we discuss the characteristics of the PDW observed in Fig. 2 in detail.

FIG. 2. PDW observed in a sample showing an LS type WB.



Let us start our discussion from the initiation stage of the PDW. The fact that the  $u$ -wave sharply rises indicates that it is initiated by an instantaneous event. In the mesomechanical picture, this can be explained as follows. When the stress reaches about 85% of the proof stress, the shear stability is lost at a certain location of the sample causing a translational displacement. Considering that the  $u$ -wave travels upwards and that Ludars bands are generally initiated near one of the tensile machine's grips in low-carbon steel [15], this location is likely to be near the lower grip of the tensile machine. By the TRI mechanism, this translational displacement induces an oscillatory motion in a neighboring DSE and the same process is repeated through a series of DSEs.

Thus the PDW starts its life as a wave whose characteristics keep changing as the deformation progresses. Around the first peak of the  $u$ -wave in Fig.2, a time delay is observed among different reference points, indicating that the PDW is traveling at this stage. Fig.3 shows the times when different reference points reach their peaks respectively. From the slope of this plot, the phase velocity can be estimated to be 110 mm/min. This value is three orders of magnitude higher than the tensile speed, and interestingly, is close to the velocity of dynamic WBs (see below). From the temporal variation observed in Fig.2, on the other hand, the period of this  $u$ -wave is estimated to be 5.2 min. Then, from this period and the above-estimated phase velocity, the wavelength of the  $u$ -wave is estimated to be 572 mm.

We carried out the same measurement for other samples of the same material and size at various tensile speeds, and estimated the phase velocity, the period and the wavelength of the measured  $u$ -waves in the same way as above. Table 1 summarizes the results comparing them with the similar estimations previously made by V. I. Danilov et. al. for the shear ( $\epsilon_{xy}$ )-waves that they observed in polycrystalline aluminum [7] and amorphous alloy  $\text{Fe}_{40}\text{Ni}_{40}\text{B}_{20}$  [6]. (The phase velocity for the polycrystalline aluminum shown in this table has been estimated from the wavelength and

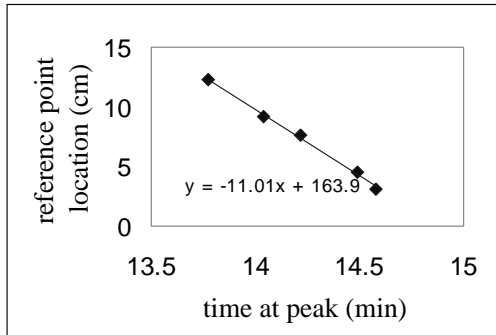
period that the authors indicate in ref. [7]. Note that in the same reference, the authors derive a phase velocity of 0.9 mm/min for the same shear-wave by a different method.) The following points should be noted in Table1. (1) the periods observed in all the cases are similar to each other, ranging from 2 to 5.2 min, regardless of the difference in the tensile speed or the material, and whether the period is estimated in a u-wave or a shear-wave; (2) all the phase velocities estimated in the u-waves in this work are similar to each other irrelevant to the tensile speed; (3) these phase velocities are, however, one to two orders of magnitude high than those estimated by V. I. Danilov et. al. [6,7] in the shear-waves; (4) in accordance with (1) and (3), the wavelength estimated in the u-waves in this work are one to two orders of magnitude longer than those of the shear-waves estimated by V. I. Danilov et. al. [6,7].

From these points, the following can be said. (1) and (2) imply that as a self-organized wave, the temporal oscillatory motion of the deforming sample is characterized by the nature of the material rather than the external force that triggers the self-organization, and that this nature is similar among the different materials listed in Table1. The observed similarity between the periods of the u-waves and the shear-waves can be explained as follows: being a spatial partial-derivative of displacement  $V(u, v)$ , shear  $\epsilon_{xy}$  should have the same temporal variation as  $V(u, v)$ , and on the other hand, being the components of the same displacement,  $u$  and  $v$  should have the same temporal variation. (Imagine  $u$  and  $v$  in the form of  $A(x, y)exp[2\pi i(\frac{t}{\tau} - \frac{x}{\lambda_x} - \frac{y}{\lambda_y})]$ , derive  $\epsilon_{xy} = \frac{1}{2}(\frac{\partial v}{\partial x} + \frac{\partial u}{\partial y})$  and see that the period of  $\epsilon_{xy}$  is still  $\tau$ .) Concerning (3) and (4), it seems more reasonable to interpret that the observed difference in the phase velocity (between our case and the Danilov's case) is caused by the difference in the wavelength, rather than the difference in the phase velocity causes the difference in the wavelength. Moreover, considering that previously in an aluminum alloy sample (A5052) of the same size we observed shear-waves having wavelengths in the order of 10 mm while the wavelength of the corresponding displacement ( $u$ ) was longer than the sample length of 200 mm [10], this difference in wavelength seems to come from the fact that we estimated the wavelength in u-waves and V. I. Danilov et. al. estimated it in shear-waves. Note that in the analogy to the Maxwell theory, the wavelength in displacement and that in distortion correspond to the wavelength and the spatial periodicity of the gradient, respectively, of an electric-magnetic field in a medium, which are fundamentally different in their physical meanings.

While the fundamental difference between the PDWs observed in displacement and distortion is a subject of future investigation, it is interesting to analyze the wavelength of the u-waves observed in this work in the same way as V. I. Danilov et. al. [7] do for the shear-wave they observed. In ref. [7], they derive the relationship between the wavelength  $\lambda$  and the grain size  $s$  as  $\lambda = L \ln(s/s_0)$ , where  $s_0$  is the minimum grain size that causes wave characteristics in the shear, and states that the value of  $L$  is associated with the characteristic length of the sample. In ref. [6] they state that the wavelength of the shear-wave observed in an amorphous alloy  $Fe_{40}Ni_{40}B_{20}$  is a linear function of the sample width, implying that the sample width is the characteristics length in that case. Considering that u-waves and the corresponding shear-waves are caused by the same self-organized phenomenon and that the grain size is a key factor determining the characteristics of the phenomenon, it will be reasonable to derive the characteristic length for our u-waves using the same formula and  $s_0$  as in ref. [7]. Thus we have derived  $L$  for our cases and list them in Table 1. It is interesting to note that the derived  $L$ 's are close to the effective length of the sample. This

result implies that for the u-waves observed in this work the longitudinal sample length is the characteristic length, and this is consistent with our intuitive interpretation that the sample swings as two rigid bodies in the final stage of deformation (see below).

FIG. 3. Phase delay observed around yield point.



After the yield point the phase delay fades out and the PDW starts to decay. Let us envision this stage of PD in the mesomechanical picture. In this stage, the scale level of the PD becomes comparable to the sample size, and consequently, the deformation becomes concentrated where the stress is highest, generating strain localization at that point. At both sides of this strain-localized point, the material tends to move as a rigid body. This situation causes the sample to swing as if it is a string vibrating in the fundamental mode, where the strain-localized point corresponds to the peak and the points gripped by the tensile machine correspond to the node of the vibration. This gives an intuitive explanation why the PDW becomes a standing wave having a wavelength roughly twice of the sample size (Table 1). As the degree of the localized strain increases the material loses the recoverability and the oscillation decays.

The decaying characteristics observed in Fig. 2 appears rather simple. It looks like the decaying motion of a simple oscillator except that the period tends to increase as the oscillation decays and the decay rate seems slightly higher than an exponential decay. It is interesting to consider this observation from the viewpoint of fluctuation dissipation theorem. In such a picture, decaying oscillation can be modeled by free vibration of a mass  $m$  hanging from a spring of a complex spring constant  $k(1 + i\phi)$  (Fig. 2). Here the real part of the spring constant represents the recoverability and the imaginary part represents the dissipation [16]. The period of the oscillation is  $\sqrt{m/k}$  and the decay constant is  $\phi/2\sqrt{k/m}$ . In such a system, if  $k$  decreases slowly and  $\phi$  increases slightly as the time elapses, it can result in the type of decay observed in Fig. 2. In our case, since the elasticity causes the recoverability and the plasticity causes the dissipation, this situation corresponds to the temporal change of the material where the elasticity decreases and plasticity increase as the deformation progresses.

It is of great interest to take a close look at Fig. 2 around the yield point. The yield point is reached as soon as the most delayed u-wave (P1) reaches its peak. This indicates that the yield occurs when this reference point swings to a side at the maximum velocity. From the viewpoint of fluctuation dissipation theorem, a peak in velocity  $u(t)$

corresponds to an equilibrium point in position  $x(t)$ . Fig. 2 clearly shows this situation, i.e., when the u-wave reaches the peak, the x-wave starts oscillating around an equilibrium point which is different from its original equilibrium point in the elastic region ( $x = 0$ ). Since a change in equilibrium is involved, the associated displacement is unrecoverable. Thermodynamically, a change in equilibrium means relaxation. These all together exactly mean that the yield point is the point where the system moves to a new equilibrium, and therefore the associated deformation is irreversible and the stress is relaxed (work hardening stops).

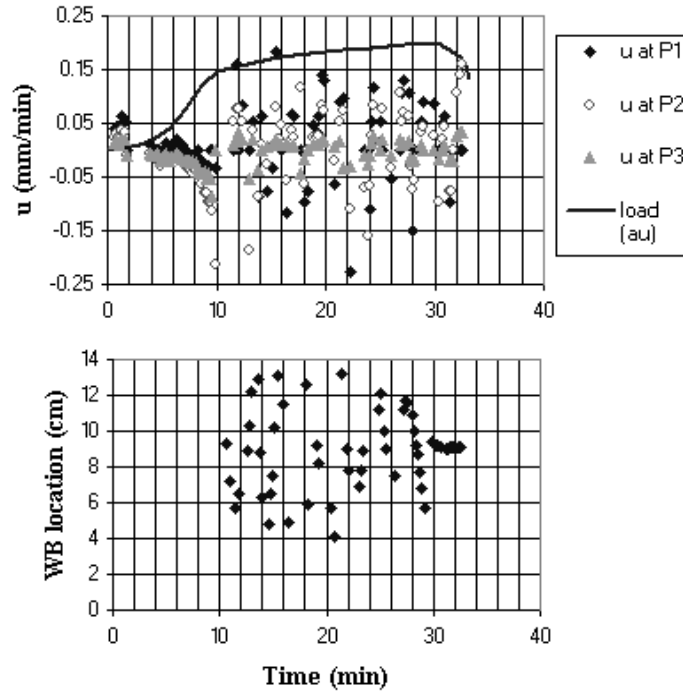
When the deformation further progresses, the material reaches the fracture stage. In the mesomechanical picture, this is the stage when the stress relaxation cannot be actualized by the dissipative nature of the PDW, but by the generation of a material discontinuity. In the fluctuation dissipation theoretical picture, this corresponds to the situation where the real part of the spring constant is too small to maintain the oscillatory character. This situation is manifested in Fig. 2 as the final part of the u-wave where it loses the oscillatory character completely. In this sample, since the fracture criterion is satisfied in the macro-level, it leads to a failure.

Now let us speculate the relationship between the PDW and the WB. In Fig. 2, the WB begins to appear at  $t = 19.6$  min when the u-wave shows the final peak before it loses its oscillatory character completely. As stated above, this is when the fracture criterion is satisfied. Our previous observation indicates that a WB is formed at the boundary of a pair of highly developed vortexes where concentrated deformation causes a large-scale slide [10]. From these facts it is reasonable to interpret that when deformation develops to the level of meso- or macro-scale fracture criterion, a slide occurs at the boundary of two developed vortexes as the alternative mechanism of stress relaxation and this slide is manifested as a WB. Since the occurrence of such a slide is instantaneous, the associated stress relaxation is also abrupt. This is consistent with our previous observation that the appearance of a WB is accompanied by an abrupt decrease in stress [10].

When the sample shows an MS type WB, the u-wave is not as simple as Fig. 2. Fig. 4 shows a typical u-wave observed in such a sample. This sample is the same as Fig. 2 in the material but is thicker (2 mm) (Often a material showing a stationary type WB as a thin sample shows an MS type WB when the sample is made thicker.) As Fig.2, the u-wave rises around the yield point, but unlike Fig.2, it does not decay monotonically. Interestingly, the traveling speed of the WB is similar to the phase velocity of the u-wave shown in Table 1 (the WB takes 1 - 2 min to travel for about 10 cm). We have not fully understood the reason for this similarity, but a possible explanation is as follows: in a sample showing a dynamic WB, first a PDW is generated somewhere in the material and travels. As soon as the fracture criterion is satisfied at a certain location, the PDW becomes stationary and a WB appears there. Since the scale-level of this fracture is not large, the material recovers from the discontinuous situation. Accordingly, the stress restarts to increase, and a new PDW starts traveling from that location to repeat the same process. This interpretation is consistent with our previous observation that the appearance of dynamic WB coincides with the zigzag characteristic of the loading curve [10]. (The zigzag characteristics are not seen in Fig. 4 because the scale is too small.)



FIG. 4. PDW and dynamic WB.



In summary, we have observed u-waves in aluminum-alloy samples under tensile loads. The u-waves observed in the samples showing an LS type WB have fairly simple oscillatory characteristics and show the pre-fracture behavior as explained by mesomechanics. The periods observed in these u-waves are similar to those of the previously observed shear-waves, while the wavelengths, hence the phase velocities, of these u-waves are one to two orders of magnitudes higher than the same previous shear-waves. The observed decaying characteristics of PDW can be intuitively understood as a relaxation process in a dissipative medium.

This work was supported by the Japanese Science and Technology Corporation. Part of the experiment was carried out at the Reactor Safety Technology Research Center of Indonesian National Atomic Agency, and metallurgical analyses of the samples were made in the laboratory of metallurgy of Indonesian Institute of Sciences. We thank Malik Rakhmanov for his helpful discussion. Suggestions and advices by Prof. V. E. Panin are highly appreciated.

- 
- [1] V. E. Panin in Physical Mesomechanics and Computer-aided Design of Materials, edited by V. E. Panin, Vol.1, (Nauka, Novosibirsk, 1995) (Russian).
  - [2] V. E. Egorshkin, Phisica, Izvestia, 33, 51 (1990) (Russian).
  - [3] V. E. Panin: Oyobuturi 64, 889 (1995).

- [4] S. Yoshida et al. in Proc. 10th Int. Conf. on the Strength of Materials, Sendai, August 1994 (The Japan Institute of Metals, Japan, 1994) p. 295.
- [5] V. Ye. Panin, L. B.Zuyev, V. I. Danilov, and N. M. Mnikh, Phys, Met. Metall, 66, 160 (1988)
- [6] V. I. Danilov, V. Ye. Panin, N. M. Mnikh and L. B.Zuyev, Phys, Met. Metall, 69, 181 (1990)
- [7] V. I. Danilov, L. B.Zuyev, N. M. Mnikh, V. Ye. Paninand and L. V. Shershova, Phys, Met. Metall, 71, 187 (1991)
- [8] V. E. Panin and V. S. Pleshanov, in Physical Mesomechanics and Computer-aided Design of Materials, edited by V. E. Panin, Vol.1 (Nauka, Novosibirsk, 1995), p. 241 (Russian).
- [9] P. V. Makarov, Phisica, Izvestia, 35, 42 (1992) (Russian).
- [10] S. Yoshida et al. Theor. and Appl. Fract. Mechanics, 27, 85 (1997).
- [11] Sanichiro Yoshida et al. Jpn. J. Appl. Phys. 35, L854 (1996).
- [12] S. Yoshida et al. Optics Express, 2, 516 (1998).
- [13] O. J. Lokberg, in Speckle Metrology, edited by R. S. Sirohi, Optical EngineeringVol. Vol. 38 (Marcel Dekker, New York, 1993), p. 163.
- [14] J. A. Leendertz, J. Phys. E 3, 214 (1970).
- [15] V. I. Danilov, L. B. Zuev and V. E. Panin, in Structural Level of Plastic Deformation and Fracture, edited by V. E. Panin (Nauka, Novosibirsk, 1990) p. 68 (Russian).
- [16] A. S. Nowick and B. S. Berry, Anelastic Relaxations in Crystalline Solids (Academic Press, New York, 1972) P. 18.

TABLE I. PDW observed at various tensile speeds and materials

tensile speed (mm/min)	phase velocity (mm/min)	period (min)	wavelength (mm)	material	L (mm)	PDW	ref
0.1	110	5.4	572	A6063	161	u-wave	this work
0.35	83	3.6	299	A6063	84.4	u-wave	this work
1.0	118	3.5	413	A6063	117	u-wave	this work
0.1	6.6	2.9	19.4	A85	2.5	shear-wave	[7]
0.09	2	2.0	4	Fe <sub>40</sub> Ni <sub>40</sub> B <sub>20</sub>	-	shear-wave	[6]